Virtual QCD corrections to Higgs boson plus four parton processes

R. K. Ellis,[*] W. T. Giele,[†] and G. Zanderighi[‡]

Fermilab, Batavia, Illinois 60510, USA
(Received 28 June 2005; published 23 September 2005)

We report on the calculation of virtual processes contributing to the production of a Higgs boson and two jets in hadron-hadron collisions. The coupling of the Higgs boson to gluons, via a virtual loop of top quarks, is treated using an effective theory, valid in the large top quark mass limit. The calculation is performed by evaluating one-loop diagrams in the effective theory. The primary method of calculation is a numerical evaluation of the virtual amplitudes as a Laurent series in $D - 4$, where D is the dimensionality of space-time. For the cases $H \to q\bar{q}q\bar{q}$ and $H \to q\bar{q}q'\bar{q}'$ we confirm the numerical results by an explicit analytic calculation.

I. INTRODUCTION

In this paper we study the production of a standard model Higgs boson in association with two jets. This is one of the most promising discovery channels at the LHC, especially for a Higgs boson with a mass in the range 110 GeV $< M_H <$ 180 GeV. At Born level there are two classes of processes which contribute, as illustrated in Fig. 1.

In Fig. 1(a), the Higgs is produced via vector boson fusion, while in Fig. 1(b) the coupling of the Higgs boson to gluons is mediated by a top quark loop. In the limit in which the mass of the top quark tends to infinity the coupling can be treated using an effective theory as described below. We shall refer to this process as the gluon fusion process. Notice that the external gluon lines in Fig. 1(b) could as well be replaced by quarks.

The final aim of this study is the calculation of the Higgs +2-jet rate, at next-to-leading order (NLO), where the Higgs is produced using the effective coupling to gluons,

$$\mathcal{L}_{\text{eff}} = \frac{1}{4} A(1 + \Delta) H G_{\mu\nu}^a G^{a\mu\nu}. \tag{1}$$

In Eq. (1), $G_{\mu\nu}^a$ is the field strength of the gluon field and H is the Higgs boson field. The effective coupling A is given by

$$A = \frac{g^2}{12\pi^2 v}, \tag{2}$$

where g is the bare strong coupling and v is the vacuum expectation value parameter, $v^2 = (G_F\sqrt{2})^{-1} = (246 \text{ GeV})^2$. The finite $O(g^2)$ correction to the effective operator has been calculated [1,2]

$$\Delta = \frac{11g^2}{16\pi^2}. \tag{3}$$

The full NLO result will require the evaluation of the

virtual corrections to the Higgs + 4 parton processes, which are the subject of this paper, the calculation of the tree graph rates from the Higgs + 5 partons amplitudes already given in Refs. [3–5] and the calculation of a set of subtraction terms. The subtractions remove singularities present in the real emission diagrams in the regions of soft and collinear emission. After integration over the momentum of the unobserved parton they are added back to the virtual emission diagrams and cancel the singularities in those virtual terms.

We believe this calculation would be a useful addition to the literature for several reasons. First, the effective Lagrangian approach appears to be valid for light Higgs boson mass if the transverse momentum of the associated jets is less than the top quark mass [6,7]. Second, this process constitutes a ''background'' to the experimentally interesting vector boson fusion process, Fig. 1(a). A complete NLO calculation will improve knowledge of this ''background'' process. In addition, because the vector boson fusion process has a well-determined normalization, it is one of the most accurate sources of information about the couplings of the Higgs boson at the LHC [8]. An uncontrolled background from gluon fusion process could compromise that measurement. For a comprehensive review of standard model Higgs physics, see Ref. [9].

[*]Electronic address: ellis@fnal.gov
[†]Electronic address: giele@fnal.gov
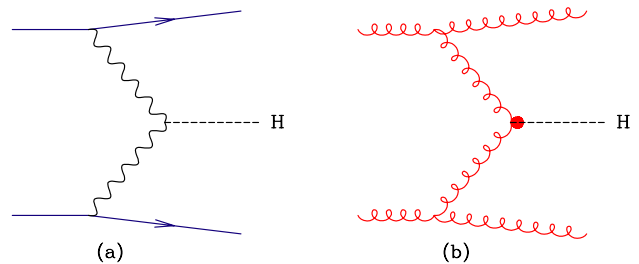[‡]Electronic address: zanderi@fnal.gov

FIG. 1 (color online). (a) Lowest order process for vector boson fusion. (b) Example of a diagram contributing to the gluon fusion process in association with two jets.

Note that the process calculated in this paper is distinguished from the vector boson process, Fig. 1(a), by the presence of colored particles exchanged in the *t*-channel. The exchange of color charge generates extra jet activity in the central region, allowing discrimination against this process by a jet veto. Although the efficacy of such a veto will finally have to be determined by experiment, it will still be interesting to see how this works at the parton level with a full NLO calculation.[1]

In the large top quark mass limit, virtual corrections have been considered in the effective theory by previous authors. Loop corrections to the process $H \to gg$ are considered at one-loop level in Ref. [1] and at two-loop level in Refs. [10,11]. The results for the processes $H \to ggg$ and $H \to q\bar{q}g$ are given in Refs. [12,13]. In the following we shall describe results for the virtual corrections to the processes

(A) $$H \to q\bar{q}q'\bar{q}', \qquad (4)$$

(B) $$H \to q\bar{q}q\bar{q}, \qquad (5)$$

(C) $$H \to q\bar{q}gg, \qquad (6)$$

(D) $$H \to gggg, \qquad (7)$$

using the effective theory, Eq. (1).

II. LOWEST ORDER PROCESS

A. $H \to q\bar{q}q'\bar{q}'$

We first perform the calculation of the matrix element for the process involving two distinct flavors of massless quarks, q and q', process A,

$$H \to q(k_1) + \bar{q}(k_2) + q'(k_3) + \bar{q}'(k_4). \qquad (8)$$

At Born level, only the diagram in Fig. 2(a) contributes. The color expansion of the amplitude can be written as

$$M_0^A(k_1, k_2, k_3, k_4) = \left[\delta_{i_4}^{i_1} \delta_{i_2}^{i_3} - \frac{1}{N_c} \delta_{i_2}^{i_1} \delta_{i_4}^{i_3} \right] a^{(0)}(1, 2, 3, 4), \qquad (9)$$

where i_j denotes the color index of the *j*th quark and we have introduced the notation

$$a^{(0)}(1, 2, 3, 4) \equiv a^{(0)}(k_1, h_1; k_2, h_2; k_3, h_3; k_4, h_4), \qquad (10)$$

where k_i and h_i denote the momentum and the helicity of quark i. The result for the squared matrix element summed over the spins and colors of the final state quarks and antiquarks is then

[1]To a limited extent this has been looked at in Ref. [3]. However in a tree graph calculation one cannot look at the effects of finite jet size or of the central jet veto.
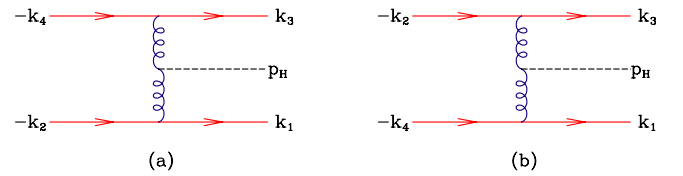

FIG. 2 (color online). (a) Lowest order process for $H \to q\bar{q}q'\bar{q}'$. (b) Second diagram for identical quark process $H \to q\bar{q}q\bar{q}$.

$$A_0(k_1, k_2, k_3, k_4) \equiv \sum |M_0^A(k_1, k_2, k_3, k_4)|^2$$

$$= g^4 A^2 V \left[\frac{(s_{13}s_{24} - s_{23}s_{14})^2 + s_{12}^2 s_{34}^2}{s_{34}^2 s_{12}^2} \right.$$

$$\left. + \frac{(s_{13} - s_{24})^2 + (s_{14} - s_{23})^2}{2s_{34}s_{12}} \right]. \qquad (11)$$

The number of colors N_c enters as $V = N_c^2 - 1$, so, for the case of SU(3), we have that $V = 8$. The Lorentz invariants are defined as $s_{ij} \equiv (k_i + k_j)^2 = 2k_i \cdot k_j$. The momentum of the Higgs can be eliminated in terms of the four massless momenta, $p_H = -k_1 - k_2 - k_3 - k_4$, so that

$$M_H^2 = s_{12} + s_{13} + s_{14} + s_{23} + s_{24} + s_{34}. \qquad (12)$$

B. $H \to q\bar{q}q\bar{q}$

In the case of massless quarks of identical flavor, process B,

$$H \to q(k_1) + \bar{q}(k_2) + q(k_3) + \bar{q}(k_4), \qquad (13)$$

the Born amplitude squared is determined by the two diagrams, shown in Fig. 2(a) and 2(b), which differ by the exchange of the final state antiquarks. The color expansion of the amplitude can be written as

$$M_0^B(k_1, k_2, k_3, k_4) = \left[\delta_{i_4}^{i_1} \delta_{i_2}^{i_3} - \frac{1}{N_c} \delta_{i_2}^{i_1} \delta_{i_4}^{i_3} \right] a^{(0)}(1, 2, 3, 4)$$

$$- \left[\delta_{i_2}^{i_1} \delta_{i_4}^{i_3} - \frac{1}{N_c} \delta_{i_4}^{i_1} \delta_{i_2}^{i_3} \right] a^{(0)}(1, 4, 3, 2)$$

$$= M_0^A(k_1, k_2, k_3, k_4) - M_0^A(k_1, k_4, k_3, k_2). \qquad (14)$$

The result for the matrix element squared, summed over the spins and colors of the final state quarks and antiquarks is given by

$$B_0(k_1, k_2, k_3, k_4) \equiv \sum |M_0^B(k_1, k_2, k_3, k_4)|^2$$

$$= A_0(k_1, k_2, k_3, k_4) + A_0(k_1, k_4, k_3, k_2)$$

$$+ B_0'(k_1, k_2, k_3, k_4), \qquad (15)$$

where the interference term is defined as

$$B_0'(k_1, k_2, k_3, k_4) \equiv -2 \sum \text{Re}[M_0^A(k_1, k_2, k_3, k_4)^\star$$

$$\times M_0^A(k_1, k_4, k_3, k_2)]. \tag{16}$$

The result for the lowest order interference term B_0' is given by,

$$B_0'(k_1, k_2, k_3, k_4) = g^4 A^2 C_f \{[(s_{13} - s_{24})^2(s_{12}s_{34} + s_{14}s_{23}$$
$$- s_{13}s_{24}) - 2(s_{13}s_{24} + s_{14}s_{23} - s_{12}s_{34})$$
$$\times (s_{12}s_{34} + s_{13}s_{24} - s_{14}s_{23})]\}$$
$$\times \frac{1}{s_{12}s_{14}s_{23}s_{34}}, \tag{17}$$

with $C_f = (N_c^2 - 1)/(2N_c) = 4/3$.

C. $H \rightarrow q\bar{q}gg$

We now turn to process C,

$$H \rightarrow q(k_1) + \bar{q}(k_2) + g(k_3) + g(k_4). \tag{18}$$

At lowest order the amplitude is given by

$$M_0^C = (T^{a_3}T^{a_4})_{i_1 i_2} c_1^{(0)}(1, 2, 3, 4)$$
$$+ (T^{a_4}T^{a_3})_{i_1 i_2} c_2^{(0)}(1, 2, 3, 4), \tag{19}$$

where a_3, a_4 are the color indices of the gluons and i_1, i_2 are the color indices of the quarks. As before we have introduced notation of the form

$$c_i^{(0)}(1, 2, 3, 4) \equiv c_i^{(0)}(k_1, h_1; k_2, h_2; k_3, \varepsilon_3; k_4, \varepsilon_4), \tag{20}$$

where ε_i is the polarization vector of gluon i and $c_2^{(0)}(1, 2, 3, 4) = c_1^{(0)}(1, 2, 4, 3)$. Explicit forms for the three independent helicity amplitudes can be found, for example, in Refs. [3,14]. The former reference also contains explicit results for the amplitude squared.

D. $H \rightarrow gggg$

Lastly we consider the matrix element for the process D,

$$H \rightarrow g(k_1) + g(k_2) + g(k_3) + g(k_4). \tag{21}$$

At lowest order the four gluon matrix element has the structure

$$M_0^D = \sum_{\sigma \in S_4/Z_4} \text{tr}(T^{a_{\sigma(1)}} T^{a_{\sigma(2)}} T^{a_{\sigma(3)}} T^{a_{\sigma(4)}})$$
$$\times d_1^{(0)}(\sigma(1), \sigma(2), \sigma(3), \sigma(4)), \tag{22}$$

where the sum runs over the six noncyclic permutations and we have introduced the notation

$$d_i(1, 2, 3, 4) \equiv d_i(k_1, \varepsilon_1; k_2, \varepsilon_2; k_3, \varepsilon_3; k_4, \varepsilon_4). \tag{23}$$

The partial amplitudes satisfy the relations [15,16]

$$d_i^{(0)}(1, 2, 3, 4) = d_i^{(0)}(4, 1, 2, 3) \quad \text{cyclicity}, \tag{24}$$

$$d_i^{(0)}(1, 2, 3, 4) = d_i^{(0)}(4, 3, 2, 1) \quad \text{reflection}, \tag{25}$$

$$d_i^{(0)}(1, 2, 3, 4) + d_i^{(0)}(2, 1, 3, 4) + d_i^{(0)}(2, 3, 1, 4) = 0 \tag{26}$$

dual Ward identity,

so that at Born level for fixed helicities there are only two independent amplitudes. Explicit expressions for the helicity amplitudes can be found, for example, in Refs. [3,14]. The former reference also contains explicit results for the amplitude squared. Equations (24) and (25) continue to be valid beyond leading order [17].

III. HIGHER ORDER PROCESSES

In order to control the divergences which will occur at higher order, we will continue the dimensionality of space-time, $D = 4 - 2\epsilon$. Within the context of dimensional regularization there remain choices of the dimensionality of internal and external gluons which are needed to completely specify the scheme. The most commonly adopted choices are the conventional dimensional regularization, (CDR), the 't Hooft-Veltman scheme, (HV) [18], and the four-dimensional helicity scheme, (FDH) [19,20]. In the CDR scheme one uniformly continues all momenta and polarization vectors to D dimensions. The HV scheme differs in the treatment of the external states, which remain four-dimensional. Finally in the FDH scheme all states are four-dimensional, and only the internal loop momenta are continued to D dimensions.

Since we are interested in a numerical evaluation of helicity amplitudes, it is preferable to consider the external quarks and gluons in four dimensions, with two physical helicity states. We choose to work in the 't Hooft-Veltman scheme. The relationship of the CDR, HV and FDH regularization schemes has been presented in Refs. [21,22]. It is therefore straightforward to translate our results to another scheme. The details of the translation between the HV and FDH schemes are provided in Sec. IV.

A. Distinct quarks

At next-to-leading order in the perturbative expansion, 30 virtual diagrams contribute to the amplitude given in Eq. (8). At one-loop level the amplitude can be decomposed into two independent color structures,

$$M_1^A(k_1, k_2, k_3, k_4) = \left[\delta_{i_4}^{i_1} \delta_{i_2}^{i_3} - \frac{1}{N_c} \delta_{i_2}^{i_1} \delta_{i_4}^{i_3} \right] a_1^{(1)}(1, 2, 3, 4)$$
$$+ \delta_{i_2}^{i_1} \delta_{i_4}^{i_3} a_2^{(1)}(1, 2, 3, 4). \tag{27}$$

The color subamplitude $a_2^{(1)}$ does not contribute at next-to-leading order because the interference with the color structure of the Born amplitude vanishes.

Before renormalization we find for the squared matrix element, summed over spin and colors of the final state

$$A_1(k_1, k_2, k_3, k_4) \equiv \sum (|M_0^A + M_1^A|^2 - |M_1^A|^2)$$

$$= A_0(k_1, k_2, k_3, k_4)\left[1 + \frac{g^2}{8\pi^2}Y^A(k_1, k_2, k_3, k_4)\right] + A^2V\frac{g^6}{8\pi^2}[X^A(k_1, k_2, k_3, k_4)$$

$$+ X^A(k_3, k_4, k_1, k_2) + X^A(k_2, k_1, k_4, k_3) + X^A(k_4, k_3, k_2, k_1)] + O(\epsilon). \tag{28}$$

All ultraviolet and infrared singularities are in the functions $Y(k_1, k_2, k_3, k_4)$ given by

$$Y^A(k_1, k_2, k_3, k_4) = -N_c\frac{c_\Gamma\mu^{2\epsilon}}{\epsilon^2}[(-s_{14})^{-\epsilon} + (-s_{23})^{-\epsilon}] + \frac{1}{N_c}\frac{c_\Gamma\mu^{2\epsilon}}{\epsilon^2}[(-s_{12})^{-\epsilon} + (-s_{34})^{-\epsilon} - 2(-s_{13})^{-\epsilon} + 2(-s_{14})^{-\epsilon}$$

$$+ 2(-s_{23})^{-\epsilon} - 2(-s_{24})^{-\epsilon})] - \frac{c_\Gamma\mu^{2\epsilon}}{\epsilon}[3C_f - b_0][(-s_{12})^{-\epsilon} + (-s_{34})^{-\epsilon}] - \frac{20}{9}n_f + \frac{152}{9}N_c - 16C_f$$

$$+ \frac{1}{N_c}[\mathrm{Ls}_{-1}^{2me}(s_{134}, s_{234}; s_{34}, M_H^2) + \mathrm{Ls}_{-1}^{2me}(s_{123}, s_{124}; s_{12}, M_H^2)] - \frac{2}{N_c}[\mathrm{Ls}_{-1}^{2me}(s_{123}, s_{134}; s_{13}, M_H^2)$$

$$+ \mathrm{Ls}_{-1}^{2me}(s_{124}, s_{234}; s_{24}, M_H^2)] - \left(N_c - \frac{2}{N_c}\right)[\mathrm{Ls}_{-1}^{2me}(s_{124}, s_{134}; s_{14}, M_H^2) + \mathrm{Ls}_{-1}^{2me}(s_{123}, s_{234}; s_{23}, M_H^2)], \tag{29}$$

where

$$c_\Gamma \equiv (4\pi)^\epsilon\frac{\Gamma(1 + \epsilon)\Gamma^2(1 - \epsilon)}{\Gamma(1 - 2\epsilon)} = \frac{(4\pi)^\epsilon}{\Gamma(1 - \epsilon)} + O(\epsilon^3), \tag{30}$$

and

$$b_0 = \left(\frac{11N_c}{3} - \frac{2n_f}{3}\right). \tag{31}$$

As usual n_f is the number of light flavors and μ is the scale introduced to keep the coupling constant dimensionless in D dimensions.

The finite function $X^A(k_1, k_2, k_3, k_4)$ is given by

$$X^A(k_1, k_2, k_3, k_4) = \mathrm{Ls}_{-1}(s_{12}, s_{13}; s_{123})\frac{2}{N_c}f_1(k_2, k_1, k_3, k_4) + \mathrm{Ls}_{-1}(s_{12}, s_{23}; s_{123})\left(N_c - \frac{2}{Nc}\right)f_1(k_1, k_2, k_3, k_4)$$

$$+ \left(\frac{1}{N_c} + N_c\right)\mathrm{L}_1\left(\frac{-s_{123}}{-s_{12}}\right)f_2(k_1, k_2, k_3, k_4) + N_c\mathrm{L}_0\left(\frac{-s_{123}}{-s_{12}}\right)f_3(k_1, k_2, k_3, k_4)$$

$$+ \frac{1}{N_c}\mathrm{L}_0\left(\frac{-s_{123}}{-s_{12}}\right)f_4(k_1, k_2, k_3, k_4) + \left(-\frac{N_c}{2} + \frac{1}{N_c}\right)\mathrm{L}_0\left(\frac{-s_{123}}{-s_{12}}\right)f_5(k_1, k_2, k_3, k_4)$$

$$- \frac{1}{N_c}\mathrm{L}_0\left(\frac{-s_{123}}{-s_{13}}\right)f_5(k_1, k_2, k_4, k_3) + N_c\ln\left(\frac{-s_{123}}{-s_{12}}\right)f_6(k_1, k_2, k_3, k_4) + N_c\ln\left(\frac{-s_{123}}{-s_{23}}\right)f_7(k_1, k_2, k_3, k_4)$$

$$+ N_c\ln\left(\frac{-s_{12}}{-s_{14}}\right)f_8(k_1, k_2, k_3, k_4) + \frac{1}{N_c}\ln\left(\frac{-s_{123}}{-s_{12}}\right)f_9(k_1, k_2, k_3, k_4) + \frac{1}{N_c}\ln\left(\frac{-s_{123}}{-s_{13}}\right)f_{10}(k_1, k_2, k_3, k_4)$$

$$+ \frac{1}{N_c}\ln\left(\frac{-s_{12}}{-s_{13}}\right)f_{11}(k_1, k_2, k_3, k_4) - \frac{1}{N_c}\ln\left(\frac{-s_{123}}{-s_{23}}\right)f_{10}(k_2, k_1, k_3, k_4) - \frac{1}{N_c}\ln\left(\frac{-s_{12}}{-s_{13}}\right)f_{11}(k_2, k_1, k_3, k_4)$$

$$+ \left(N_c + \frac{1}{N_c}\right)f_{12}(k_1, k_2, k_3, k_4). \tag{32}$$

The special functions coming from the loop integrals, $L_0, L_1, \mathrm{Ls}_{-1}$ and Ls_{-1}^{2me} are given in Appendix A. The explicit expression for the kinematic functions f_i are given in Appendix B. We note that the line-reversal symmetry

$(1 \leftrightarrow 2$ and $3 \leftrightarrow 4)$ and the renaming property $(1 \leftrightarrow 3$ and $2 \leftrightarrow 4)$ are manifest in Eq. (28).

The ultraviolet divergences are removed in the $\overline{\mathrm{MS}}$-scheme by adding a counterterm A_{ct} given by

$$A_{ct}(k_1, k_2, k_3, k_4) = -2\frac{c_\Gamma}{\epsilon} b_0 \frac{g^2}{16\pi^2} A_0(k_1, k_2, k_3, k_4). \quad (33)$$

Additionally, there is a finite contribution, A_{fin}, coming from the effective Lagrangian, Eq. (1), which is

$$A_{fin}(k_1, k_2, k_3, k_4) = \Delta A_0(k_1, k_2, k_3, k_4), \quad (34)$$

where Δ is given in Eq. (3).

B. Identical quarks

In the case of identical quarks, 60 diagrams contribute the next-to-leading order process, Eq. (13). Before renor-

malization we find for the squared amplitude, summed over colors and spins,

$$B_1(k_1, k_2, k_3, k_4) \equiv \sum (|M_0^B + M_1^B|^2 - |M_1^B|^2) \quad (35)$$

$$= A_1(k_1, k_2, k_3, k_4) + A_1(k_1, k_4, k_3, k_2) + B_1'(k_1, k_2, k_3, k_4), \quad (36)$$

with A_1 given in (A1). The result for the interference term can be written as,

$$
\begin{aligned}
B_1'(k_1, k_2, k_3, k_4) = {} & B_0'(k_1, k_2, k_3, k_4)\left[1 + \frac{g^2}{8\pi^2} Y^B(k_1, k_2, k_3, k_4)\right] + A^2 V \frac{g^6}{8\pi^2}[X^B(k_1, k_2, k_3, k_4) + X^B(k_3, k_2, k_1, k_4) \\
& + X^B(k_1, k_4, k_3, k_2) + X^B(k_3, k_4, k_1, k_2) + X^B(k_4, k_3, k_2, k_1) + X^B(k_2, k_3, k_4, k_1) \\
& + X^B(k_4, k_1, k_2, k_3) + X^B(k_2, k_1, k_4, k_3)] + O(\epsilon),
\end{aligned}
\quad (37)
$$

where the function Y^B contains all divergent terms

$$
\begin{aligned}
Y^B(k_1, k_2, k_3, k_4) = {} & -\frac{c_\Gamma N_c \mu^{2\epsilon}}{\epsilon^2}((-s_{24})^{-\epsilon} + (-s_{13})^{-\epsilon}) + \frac{c_\Gamma \mu^{2\epsilon}}{N_c \epsilon^2}[(-s_{12})^{-\epsilon} + (-s_{34})^{-\epsilon} + (-s_{14})^{-\epsilon} + (-s_{23})^{-\epsilon} \\
& - (-s_{24})^{-\epsilon} - (-s_{13})^{-\epsilon}] + \frac{c_\Gamma \mu^{2\epsilon}}{4\epsilon}(-6C_f + 2b_0)[(-s_{12})^{-\epsilon} + (-s_{14})^{-\epsilon} + (-s_{23})^{-\epsilon} + (-s_{34})^{-\epsilon}] \\
& - \frac{20n_f}{9} + \frac{80N_c}{9} + \frac{8}{N_c} + \frac{1}{N_c}[\mathrm{Ls}_{-1}^{2me}(s_{134}, s_{234}; s_{34}, M_H^2) + \mathrm{Ls}_{-1}^{2me}(s_{123}, s_{234}; s_{23}, M_H^2) \\
& + \mathrm{Ls}_{-1}^{2me}(s_{124}, s_{134}; s_{14}, M_H^2) + \mathrm{Ls}_{-1}^{2me}(s_{123}, s_{124}; s_{12}, M_H^2)] - (N_c + \frac{1}{N_c})[\mathrm{Ls}_{-1}^{2me}(s_{123}, s_{134}; s_{13}, M_H^2) \\
& - \mathrm{Ls}_{-1}^{2me}(s_{124}, s_{234}; s_{24}, M_H^2)].
\end{aligned}
\quad (38)
$$

The finite function X^B is given by

$$
\begin{aligned}
X^B(k_1, k_2, k_3, k_4) = {} & -\mathrm{Ls}_{-1}(s_{12}, s_{13}; s_{123})g_1(s_{12}, s_{13}, s_{14}, s_{23}, s_{24}, s_{34})\left(1 + \frac{1}{N_c^2}\right) \\
& - \mathrm{Ls}_{-1}(s_{12}, s_{23}; s_{123})g_2(s_{12}, s_{13}, s_{14}, s_{23}, s_{24}, s_{34})\frac{1}{N_c^2} + \mathrm{L}_1\left(\frac{-s_{123}}{-s_{12}}\right)g_3(s_{12}, s_{13}, s_{14}, s_{23}, s_{24}, s_{34})\left(1 + \frac{1}{N_c^2}\right) \\
& + \mathrm{L}_0\left(\frac{-s_{123}}{-s_{12}}\right)g_4(s_{12}, s_{13}, s_{14}, s_{23}, s_{24}, s_{34}) + \mathrm{L}_0\left(\frac{-s_{123}}{-s_{12}}\right)g_5(s_{12}, s_{13}, s_{14}, s_{23}, s_{24}, s_{34})\frac{1}{N_c^2} \\
& + \ln\left(\frac{-s_{123}}{-s_{12}}\right)g_6(s_{12}, s_{13}, s_{14}, s_{23}, s_{24}, s_{34}) + \ln\left(\frac{-s_{123}}{-s_{12}}\right)g_7(s_{12}, s_{13}, s_{14}, s_{23}, s_{24}, s_{34})\frac{1}{N_c^2} \\
& + g_8(s_{12}, s_{13}, s_{14}, s_{23}, s_{24}, s_{34})\left(1 + \frac{1}{N_c^2}\right),
\end{aligned}
\quad (39)
$$

where the functions g_i are given in Appendix C. We note that the result in Eq. (35) is symmetric under the exchange of $(1 \leftrightarrow 3)$ or $(2 \leftrightarrow 4)$.

The counterterm renormalizing the ultraviolet divergences in the case of identical quarks reads

$$B_{ct}(k_1, k_2, k_3, k_4) = -2\frac{c_\Gamma}{\epsilon} b_0 \frac{g^2}{16\pi^2} B_0(k_1, k_2, k_3, k_4), \quad (40)$$

while the finite contribution coming from the effective

Lagrangian is

$$B_{fin}(k_1, k_2, k_3, k_4) = \Delta B_0(k_1, k_2, k_3, k_4). \quad (41)$$

C. $H \to q\bar{q}gg$

At one loop the full amplitude is calculated from 191 Feynman diagrams, which can be decomposed into the three color-ordered subamplitudes,

$$M_1^C = (T^{a_3}T^{a_4})_{i_1 i_2} c_1^{(1)}(1, 2, 3, 4)$$

$$+ (T^{a_4}T^{a_3})_{i_1 i_2} c_2^{(1)}(1, 2, 3, 4)$$

$$+ \delta^{a_3 a_4}\delta_{i_1 i_2} c_3^{(1)}(1, 2, 3, 4). \tag{42}$$

Bose symmetry requires that $c_2^{(1)}(1, 2, 3, 4) = c_1^{(1)}(1, 2, 4, 3)$.

The divergent parts of these one-loop amplitudes are given by

$$c_1^{(1)}(1, 2, 3, 4) \rightarrow c_\Gamma \frac{g^2 \mu^{2\epsilon}}{16\pi^2}\bigg[-\frac{N_c}{\epsilon^2}((-s_{24})^{-\epsilon} + (-s_{13})^{-\epsilon}$$

$$+ (-s_{34})^{-\epsilon}) + \frac{1}{N_c \epsilon^2}(-s_{12})^{-\epsilon}$$

$$- \frac{3C_f}{\epsilon} + \frac{b_0}{\epsilon}\bigg]c_1^{(0)}(1, 2, 3, 4) \tag{43}$$

$$c_3^{(1)}(1, 2, 3, 4) \rightarrow c_\Gamma \frac{g^2 \mu^{2\epsilon}}{16\pi^2}\bigg[\frac{1}{2\epsilon^2}c_1^{(0)}(1, 2, 3, 4)((-s_{14})^{-\epsilon}$$

$$+ (-s_{23})^{-\epsilon} - (-s_{12})^{-\epsilon} - (-s_{34})^{-\epsilon})$$

$$+ \frac{1}{2\epsilon^2}c_2^{(0)}(1, 2, 3, 4)((-s_{13})^{-\epsilon}$$

$$+ (-s_{24})^{-\epsilon} - (-s_{12})^{-\epsilon} - (-s_{34})^{-\epsilon})\bigg]. \tag{44}$$

The interference between the Born and the NLO amplitude is given by

$$2\text{Re}(M_1^C M_0^{C\star}) = \frac{VN_c}{2}\text{Re}[c_1^{(1)}c_1^{(0)\star} + c_2^{(1)}c_2^{(0)\star}]$$

$$- \frac{V}{2N_c}\text{Re}[(c_1^{(1)} + c_2^{(1)})(c_1^{(0)} + c_2^{(0)})^\star]$$

$$+ V\text{Re}[c_3^{(1)}(c_1^{(0)} + c_2^{(0)})^\star], \tag{45}$$

with $c_i \equiv c_i(1, 2, 3, 4)$. Counterterms, analogous to those in Eqs. (33) and (34) need to be included to obtain the full renormalized result.

Numerical results, which are given in the following section, were generated using an extension of the method suggested in Ref. [23]. Analytic expressions for the Feynman graphs are generated using Qgraf [24] and Form [25]. The scalar and tensor integrals appearing in the amplitudes are reduced numerically using the Davydychev reduction for the tensor integrals [26] and a recursive procedure similar to the one proposed in Ref. [23] to reduce all scalar integrals to a small number of analytically known basis integrals. These are then evaluated numerically as a Laurent series in the ϵ parameter.[2] The key point of this method is that a record is kept of all previously computed integrals, so that each scalar integral

is computed only once. The result of our procedure is a numerical expression for the scalar and tensor integrals component by component each of which has a Laurent expansion in ϵ. This method will be described in detail in a later paper [28]. Numerical or seminumerical methods have also been described in Refs. [27,29–36].

D. $H \rightarrow gggg$

At NLO the amplitude for process Eq. (21) requires the calculation of 739 Feynman diagrams, which can be expanded in nine color subamplitudes

$$M_1^D = \sum_{\sigma \in S_4/Z_4} \text{tr}(T^{a_{\sigma(1)}}T^{a_{\sigma(2)}}T^{a_{\sigma(3)}}T^{a_{\sigma(4)}})$$

$$\times d_1^{(1)}(\sigma(1), \sigma(2), \sigma(3), \sigma(4))$$

$$+ \frac{1}{N_c}\text{tr}(T^{a_1}T^{a_2})\text{tr}(T^{a_3}T^{a_4})d_2^{(1)}(1, 2, 3, 4)$$

$$+ \frac{1}{N_c}\text{tr}(T^{a_1}T^{a_3})\text{tr}(T^{a_2}T^{a_4})d_2^{(1)}(1, 3, 2, 4)$$

$$+ \frac{1}{N_c}\text{tr}(T^{a_1}T^{a_4})\text{tr}(T^{a_2}T^{a_3})d_2^{(1)}(1, 4, 2, 3). \tag{46}$$

If we discard diagrams with internal quark loops we have the decoupling identity [17]

$$d_2^{(1)}(1, 2, 3, 4) = \sum_{\sigma \in S_4/Z_4} d_1^{(1)}(\sigma(1), \sigma(2), \sigma(3), \sigma(4)). \tag{47}$$

However, at NLO the d_2 terms in Eq. (46) do not receive contributions from internal fermion loops. This can be easily shown by explicitly examining the diagrams with internal fermionic bubbles, triangles, and boxes. The general expansion can thus be simplified as a consequence of Eq. (47) so that

$$M_1^D = \sum_{\sigma \in S_4/Z_4} \text{tr}(T^{a_{\sigma(1)}}T^{a_{\sigma(2)}}T^{a_{\sigma(3)}}T^{a_{\sigma(4)}})$$

$$\times d_1^{(1)}(\sigma(1), \sigma(2), \sigma(3), \sigma(4))$$

$$+ \frac{1}{N_c}[\text{tr}(T^{a_1}T^{a_2})\text{tr}(T^{a_3}T^{a_4}) + \text{tr}(T^{a_1}T^{a_3})\text{tr}(T^{a_2}T^{a_4})$$

$$+ \text{tr}(T^{a_1}T^{a_4})\text{tr}(T^{a_2}T^{a_3})]d_2^{(1)}(1, 2, 3, 4). \tag{48}$$

Using Eq. (48) it can be shown that the result for the matrix element squared is

$$|M_0^D + M_1^D|^2 - |M_1^D|^2 = \frac{N_c^2(N_c^2 - 1)}{16} \sum_{\sigma \in S_4/Z_4}$$

$$\times \{|d_1^{(0)}(\sigma(1), \sigma(2), \sigma(3), \sigma(4))|^2$$

$$+ 2\text{Re}[d_1^{(0)}(\sigma(1), \sigma(2), \sigma(3), \sigma(4))^\star$$

$$\times d_1^{(1)}(\sigma(1), \sigma(2), \sigma(3), \sigma(4))]\}. \tag{49}$$

Counterterms, analogous to those in Eqs. (33) and (34) need to be included to obtain the full renormalized result.

---

[2]The *numerical* Laurent expansion technique was first used in Ref. [27]. In a more general analytic context it was used by many authors before.

Numerical results for this matrix element squared were generated using the method described above. The pole structure for the color subamplitude d_1 has the simple form

$$d_1^{(1)}(1,2,3,4) \rightarrow \frac{c_\Gamma g^2 \mu^{2\epsilon}}{16\pi^2} \left[-\frac{N_c}{\epsilon^2} ((-s_{12})^{-\epsilon} + (-s_{23})^{-\epsilon} + (-s_{34})^{-\epsilon} + (-s_{14})^{-\epsilon}) \right] d_1^{(0)}(1,2,3,4).$$

(50)

IV. NUMERICAL RESULTS

In this section we present numerical results for the Born amplitude squared and for its interference with the one-loop matrix element for the four processes of interest, A, B, C, and D. We use the following arbitrarily chosen, momentum configuration, where a Higgs boson of unit mass decays into four well separated partons, (E, p_x, p_y, p_z):

$$p_H = (-1.000\,000\,000\,00, 0.000\,000\,000\,00, 0.000\,000\,000\,00, 0.000\,000\,000\,00),$$
$$k_1 = (+0.306\,740\,378\,67, -0.177\,386\,946\,93, -0.016\,644\,720\,21, -0.249\,692\,779\,74),$$
$$k_2 = (+0.344\,450\,322\,81, +0.146\,352\,828\,00, -0.107\,077\,623\,97, +0.292\,850\,229\,75),$$
$$k_3 = (+0.220\,916\,676\,41, +0.089\,119\,159\,38, +0.197\,339\,018\,56, +0.043\,809\,417\,93),$$
$$k_4 = (+0.127\,892\,622\,11, -0.058\,085\,040\,45, -0.073\,616\,674\,38, -0.086\,966\,867\,95).$$

(51)

For each process, {A, B, C, D}, we introduce the quantities

$$X_B = \frac{1}{g^4 A^2} X_0(k_1, k_2, k_3, k_4),$$

$$X_V = \frac{8\pi^2}{g^6 A^2} [X_1(k_1, k_2, k_3, k_4) - X_0(k_1, k_2, k_3, k_4)],$$

(52)

with $X = $ A, B, C, D,

which are independent of the value of the coupling constant. Thus X_B is the matrix element squared evaluated using the Born amplitude. $X_{V,N}$ and $X_{V,A}$ denote the contributions of the interference between the virtual amplitude and the lowest order, as calculated from the numerical and analytical formulas. The unrenormalized results are given

in Table I for the scale choice $\mu = M_H$ and the momenta of Eq. (51).

The explicit results show that far from exceptional momentum configurations, where divergent inverse Gram determinants are known to spoil the accuracy of the numerical procedure, a relative accuracy of $\mathcal{O}(10^{-13})$ can be achieved. For processes C and D, where a full analytical result is not available, we verified that the answer satisfies the Ward identities to a similar relative accuracy. For process D we checked numerically that for $n_f = 0$, the color amplitudes satisfy the decoupling identity, Eq. (47). Close to exceptional momentum configurations, it is still possible to use a numerical approach [28,37].

We have also checked numerically that our results satisfy the following relationship between the HV and FDH regularization schemes,

TABLE I. Numerical results for the Born amplitude squared (X_B) and the numerical and analytic one-loop corrections ($X_{V,N}$ and $X_{V,A}$) to the four processes A, B, C, D, Eqs. (4)–(7).

	c_Γ/ϵ^2	c_Γ/ϵ	1
A_B	0	0	12.916 295 821 238 7
$A_{V,N}$	−68.886 911 046 606 3	−114.642 248 172 519	120.018 444 115 458
$A_{V,A}$	−68.886 911 046 606 4	−114.642 248 172 523	120.018 444 115 429
B_B	0	0	858.856 417 157 052
$B_{V,N}$	−4580.567 558 170 94	−436.142 317 955 208	26 470.960 897 835 0
$B_{V,A}$	−4580.567 558 170 99	−436.142 317 955 660	26 470.960 897 834 6
C_B	0	0	968.590 160 211 857
$C_{V,N}$	−8394.448 055 169 30	−19 808.039 633 135 4	−1287.905 749 491 12
$C_{V,A}$	−8394.448 055 169 42	−19 808.039 633 136 3	not known
D_B	0	0	3 576 991.279 608 52
$D_{V,N}$	−4.292 389 535 530 22 × 10⁷	−1.044 363 726 555 80 × 10⁸	−6.798 309 114 716 04 × 10⁷
$D_{V,A}$	−4.292 389 535 530 22 × 10⁷	−1.044 363 726 555 80 × 10⁸	not known

$$a_1^{(1)\mathrm{FDH}}(1,2,3,4) - a_1^{(1)\mathrm{HV}}(1,2,3,4) = \frac{g^2}{16\pi^2}\left(\frac{N_c}{3} - \frac{1}{N_c}\right)a^{(0)}(1,2,3,4), \qquad a_2^{(1)\mathrm{FDH}}(1,2,3,4) - a_2^{(1)\mathrm{HV}}(1,2,3,4) = 0,$$
$$\tag{53}$$
$$c_1^{(1)\mathrm{FDH}}(1,2,3,4) - c_1^{(1)\mathrm{HV}}(1,2,3,4) = \frac{g^2}{16\pi^2}\left(\frac{N_c}{6} - \frac{1}{2N_c}\right)c_1^{(0)}(1,2,3,4), \qquad c_3^{(1)\mathrm{FDH}}(1,2,3,4) - c_3^{(1)\mathrm{HV}}(1,2,3,4) = 0,$$
$$d_1^{(1)\mathrm{FDH}}(1,2,3,4) - d_1^{(1)\mathrm{HV}}(1,2,3,4) = 0.$$

Applying the finite renormalization which compensates for the difference between the ultraviolet regularization in the two schemes [21], we recover the expected difference between the two schemes due to the differing infrared regularization,

$$a_1^{(1)\mathrm{FDH}}(1,2,3,4) - a_1^{(1)\mathrm{HV}}(1,2,3,4)$$
$$= \frac{g^2}{4\pi^2}\tilde{\gamma}_q a^{(0)}(1,2,3,4), c_1^{(1)\mathrm{FDH}}(1,2,3,4) - c_1^{(1)\mathrm{HV}}(1,2,3,4)$$
$$= \frac{g^2}{8\pi^2}(\tilde{\gamma}_q + \tilde{\gamma}_g)c_1^{(0)}(1,2,3,4), d_1^{(1)\mathrm{FDH}}(1,2,3,4)$$
$$- d_1^{(1)\mathrm{HV}}(1,2,3,4)$$
$$= \frac{g^2}{4\pi^2}\tilde{\gamma}_g d_1^{(0)}(1,2,3,4), \tag{54}$$

where

$$\tilde{\gamma}_q \equiv \frac{C_f}{2} \quad \text{and} \quad \tilde{\gamma}_g \equiv \frac{N_c}{6}. \tag{55}$$

The other two relations in Eq. (53) are unchanged.

V. OUTLOOK

In this paper we presented results obtained using a general, seminumerical calculation of one-loop corrections. In order to establish the feasibility of the seminumerical method, we computed all the one-loop corrections to Higgs plus four parton processes using an effective Lagrangian. We presented explicit results for a specific, nonexceptional phase space point. For practical applications of this method, one has to be able to treat exceptional momentum configurations also. The method of this paper can be extended to treat those regions. A detailed description of the algorithm is presented in a separate work [28].

The results presented in this paper generate two separate lines of research. The first is clearly the completion of the calculation of the Higgs boson plus two jet process at next-to-leading order. As indicated in the text all of the needed elements are now in place.

The second development is the extension of these methods to calculate other one-loop processes which currently lie beyond the range of analytic calculation. Examples of processes of current experimental interest are diboson plus one jet (V_1, V_2, j), triboson production (V_1, V_2, V_3) and vector boson plus heavy quark pairs ($VQ\bar{Q}$).

APPENDIX A: INTEGRAL FUNCTIONS APPEARING IN AMPLITUDES

The integral functions appearing in the virtual corrections are presented in this appendix. Following closely the notation of Ref. [38] we define

$$\mathrm{L}_0(r) = \frac{\ln(r)}{1-r}, \qquad \mathrm{L}_1(r) = \frac{\mathrm{L}_0(r)+1}{1-r}. \tag{A1}$$

The above functions have the property that they are finite as their denominators vanish. Furthermore we define

$$\mathrm{Ls}_{-1}(s,t;m^2) = \mathrm{Li}_2\left(1 - \frac{s}{m^2}\right) + \mathrm{Li}_2\left(1 - \frac{t}{m^2}\right)$$
$$+ \ln\left(\frac{-s}{-m^2}\right)\ln\left(\frac{-t}{-m^2}\right) - \frac{\pi^2}{6}, \tag{A2}$$

where the dilogarithm is defined as usual as

$$\mathrm{Li}_2(x) = -\int_0^x dz\,\frac{\ln(1-z)}{z}. \tag{A3}$$

The function Ls_{-1} is simply related to the scalar box integral with one external mass evaluated in six spacetime dimensions, where it is infrared- and ultraviolet-finite.

The "easy" six-dimensional box function with two nonadjacent external masses, m_1, m_3, is related to the function $\mathrm{Ls}_{-1}^{2m e}$

$$\mathrm{Ls}_{-1}^{2m e}(s,t;m_1^2,m_3^2) = -\mathrm{Li}_2\left(1 - \frac{m_1^2}{s}\right) - \mathrm{Li}_2\left(1 - \frac{m_1^2}{t}\right)$$
$$- \mathrm{Li}_2\left(1 - \frac{m_3^2}{s}\right) - \mathrm{Li}_2\left(1 - \frac{m_3^2}{t}\right)$$
$$+ \mathrm{Li}_2\left(1 - \frac{m_1^2 m_3^2}{st}\right) - \frac{1}{2}\ln^2\left(\frac{-s}{-t}\right). \tag{A4}$$

This function has the property that it vanishes as $s + t - m_1^2 - m_3^2 \to 0$. The analytic continuation of these integrals is obtained adding a small positive imaginary part to each invariant, $s_{ij} \to s_{ij} + i\varepsilon$.

APPENDIX B: FUNCTIONS FOR DISTINCT QUARKS

The kinematic functions for the virtual corrections to $H \rightarrow q\bar{q}q'\bar{q}'$ appearing in Eq. (32) are given below:

$$f_1(k_1, k_2, k_3, k_4) = -\frac{s_{12}s_{34}}{2s_{13}^2} + \frac{3s_{13}s_{24} - s_{23}^2 + s_{14}s_{23} - s_{14}^2 - s_{13}^2}{s_{12}s_{34}} - \frac{s_{14}^2 s_{23}}{2s_{12}s_{13}^2 s_{34}} - \frac{s_{24}^2}{2s_{12}s_{34}}$$
$$- 2\frac{(s_{13}s_{24} - s_{14}s_{23})^2}{s_{12}^2 s_{34}^2} + \frac{s_{24}}{s_{13}} + \frac{s_{14}s_{23}}{s_{13}^2} - 2 \tag{B1}$$

$$f_2(k_1, k_2, k_3, k_4) = \frac{s_{12}s_{34}(s_{12}s_{34} + s_{23}(s_{24} + 2s_{23} - s_{14})) + s_{23}^2(s_{24} + s_{14})^2}{2s_{12}^3 s_{34}} \tag{B2}$$

$$f_3(k_1, k_2, k_3, k_4) = \frac{s_{34}}{2s_{23}} + s_{23}(s_{24} + s_{14})$$
$$\times \frac{s_{24} + 4s_{23} + 3s_{14}}{2s_{12}^2 s_{34}} + \frac{3s_{24} + 4s_{23}}{2s_{12}} \tag{B3}$$

$$f_4(k_1, k_2, k_3, k_4) = -2\frac{s_{34}}{s_{23}} - s_{23}(s_{24} + s_{14})$$
$$\times \frac{s_{24} + 2s_{23} + 5s_{14}}{2s_{12}^2 s_{34}}$$
$$- \frac{4s_{24} + 6s_{23} - 3s_{14}}{2s_{12}} \tag{B4}$$

$$f_5(k_1, k_2, k_3, k_4) = -\frac{s_{13}}{s_{14}} - \frac{2s_{23}}{s_{24}} + \frac{s_{24}}{s_{14}} - \frac{s_{23}}{s_{34}} - \frac{s_{14}s_{23}^2}{s_{24}^2 s_{34}}$$
$$+ \frac{s_{13}s_{23}}{s_{24}s_{34}} + \frac{s_{13}s_{24}}{s_{14}s_{34}} - \frac{s_{34}}{s_{14}} \tag{B5}$$

$$f_6(k_1, k_2, k_3, k_4) = \frac{s_{12}s_{34}}{2s_{13}s_{23}}$$
$$+ \frac{4s_{23}s_{24} + 2s_{14}s_{24} - 3s_{13}s_{24} + 3s_{14}s_{23}}{2s_{12}s_{34}}$$
$$+ \frac{s_{14}^2 s_{23}}{2s_{12}s_{13}s_{34}} - \frac{s_{14}}{s_{13}} + \frac{1}{2} \tag{B6}$$

$$f_7(k_1, k_2, k_3, k_4) = \frac{s_{14}^2 s_{23}^2 + s_{13}s_{34}^2 s_{12} - s_{13}s_{14}s_{23}s_{24}}{2s_{13}^2 s_{34}s_{12}} \tag{B7}$$

$$f_8(k_1, k_2, k_3, k_4) = \frac{s_{14}s_{23} - s_{13}s_{24}}{2s_{12}s_{34}} \tag{B8}$$

$$f_9(k_1, k_2, k_3, k_4) = \frac{s_{13}s_{24}^2}{s_{12}s_{23}s_{34}} - \frac{s_{12}s_{34}}{s_{13}s_{23}} - \frac{s_{14}^2 s_{23}}{s_{12}s_{13}s_{34}} - 2\frac{s_{24}}{s_{23}} + 2\frac{s_{14}}{s_{13}} - 1$$
$$- \frac{2s_{24}^2 + 2s_{23}s_{24} + 5s_{14}s_{24} - 5s_{13}s_{24} + 5s_{14}s_{23}}{2s_{12}s_{34}} \tag{B9}$$

$$f_{10}(k_1, k_2, k_3, k_4) = \frac{s_{12}s_{23}s_{34}^2 + s_{13}^2 s_{24}^2 - s_{13}s_{14}s_{23}s_{24}}{s_{12}s_{23}^2 s_{34}} \tag{B10}$$

$$f_{11}(k_1, k_2, k_3, k_4) = \frac{2s_{13}s_{24}}{s_{12}s_{34}} \tag{B11}$$

$$f_{12}(k_1, k_2, k_3, k_4) = \frac{s_{13}(s_{13}(s_{14} - s_{24}) + 2s_{14}s_{23})}{2s_{12}^2 s_{34}} + \frac{s_{14}}{2s_{12}}. \tag{B12}$$

APPENDIX C: FUNCTIONS FOR IDENTICAL QUARKS

The kinematic functions for the virtual corrections to $H \rightarrow q\bar{q}q\bar{q}$ appearing in Eq. (35) are given below:

$$g_1(k_1, k_2, k_3, k_4) = -1 - \frac{s_{13}s_{24}(s_{13}^2 + s_{24}^2)}{4s_{12}s_{14}s_{23}s_{34}}$$
$$+ \frac{s_{13}^2 + 2s_{14}s_{23} - 2s_{13}s_{24} + s_{24}^2}{4s_{12}s_{34}}$$
$$+ \frac{s_{13}^2 - 2s_{13}s_{24} + s_{24}^2 + 2s_{12}s_{34}}{4s_{14}s_{23}} \tag{C1}$$

$$g_2(k_1, k_2, k_3, k_4) = \frac{1}{4} - \frac{s_{24}}{4s_{13}} - \frac{s_{14}^2 s_{23}^2}{8s_{12}s_{13}^2 s_{34}} + \frac{3s_{14}s_{23}s_{24}}{8s_{12}s_{13}s_{34}} + \frac{s_{13}s_{24}(s_{13}^2 + s_{24}^2)}{4s_{12}s_{14}s_{23}s_{34}} - \frac{2s_{13}^2 + 3s_{14}s_{23} - 3s_{13}s_{24} + 4s_{24}^2}{8s_{12}s_{34}}$$

$$+ \frac{3s_{12}s_{24}s_{34}}{8s_{13}s_{14}s_{23}} - \frac{s_{12}^2 s_{34}^2}{8s_{13}^2 s_{14}s_{23}} + \frac{s_{14}s_{23} + s_{12}s_{34}}{8s_{13}^2} - \frac{2s_{13}^2 - 3s_{13}s_{24} + 4s_{24}^2 + 3s_{12}s_{34}}{8s_{14}s_{23}} \tag{C2}$$

$$g_3(k_1, k_2, k_3, k_4) = \frac{s_{23}^2 s_{24}}{8s_{12}^2 s_{14}} + \frac{s_{23}(s_{14} + s_{23} + s_{24})}{8s_{12}^2}$$

$$- \frac{s_{34}}{4s_{12}} + \frac{(s_{23} + s_{24})s_{34}}{8s_{12}s_{14}}$$

$$+ \frac{s_{34}^2}{8s_{14}s_{23}} \tag{C3}$$

$$g_5(k_1, k_2, k_3, k_4) = \frac{s_{14}}{4s_{12}} + \frac{s_{24}}{8s_{12}} - \frac{s_{24}^2}{4s_{12}s_{14}} + \frac{3s_{23}(-2s_{14} + s_{24})}{8s_{12}s_{14}}$$

$$- \frac{s_{23}(s_{14} + s_{24})^2}{4s_{12}^2 s_{34}} + \frac{s_{34}}{4s_{14}} + \frac{s_{34}}{4s_{23}} - \frac{3s_{24}s_{34}}{8s_{14}s_{23}}$$

$$- \frac{s_{12}s_{34}^2}{4s_{14}s_{23}^2} \tag{C5}$$

$$g_6(k_1, k_2, k_3, k_4) = \frac{5}{8} - \frac{s_{24}}{4s_{14}} + \frac{3s_{13}s_{24} + 4s_{24}^2 - 3s_{12}s_{34}}{8s_{14}s_{23}} \tag{C6}$$

$$g_4(k_1, k_2, k_3, k_4) = \frac{6s_{23} - 3s_{24}}{8s_{12}} + \frac{s_{24}(-s_{23} + 4s_{24})}{8s_{12}s_{14}}$$

$$- \frac{s_{34}}{4s_{14}} + \frac{5s_{24}s_{34}}{8s_{14}s_{23}} \tag{C4}$$

$$g_7(k_1, k_2, k_3, k_4) = -\frac{7}{8} + \frac{s_{14}}{4s_{13}} + \frac{s_{24}}{4s_{14}} - \frac{s_{14}^2 s_{23}}{4s_{12}s_{13}s_{34}}$$

$$- \frac{s_{24}^2}{4s_{12}s_{34}} + \frac{s_{12}s_{34}}{4s_{13}s_{23}} - \frac{s_{12}^2 s_{34}^2}{4s_{13}s_{14}s_{23}^2}$$

$$- \frac{s_{13}s_{24} + 2s_{24}^2 - s_{12}s_{34}}{8s_{14}s_{23}} \tag{C7}$$

$$g_8(k_1, k_2, k_3, k_4) = \frac{s_{12}}{32s_{14}} + \frac{s_{14}}{32s_{12}} + \frac{s_{12}}{32s_{23}} + \frac{s_{13}(s_{14} - 2s_{24})}{64s_{12}s_{23}} - \frac{s_{13}s_{24}}{32s_{12}s_{14}} + \frac{s_{13}s_{24}(s_{13} + s_{24})}{64s_{12}s_{14}s_{23}} + \frac{s_{23}(2s_{14} + s_{24})}{64s_{12}s_{14}}$$

$$+ \frac{s_{14} + s_{23}}{32s_{34}} + \frac{s_{13}(s_{12} + s_{23} - 2s_{24})}{64s_{14}s_{34}} + \frac{(s_{12} - 2s_{13} + s_{14})s_{24}}{64s_{23}s_{34}} + \frac{s_{13}s_{24}(s_{13} + s_{24})}{64s_{12}s_{14}s_{34}} + \frac{s_{13}s_{24}(s_{13} + s_{24})}{64s_{12}s_{23}s_{34}}$$

$$+ \frac{s_{13}s_{24}(s_{13} + s_{24})}{64s_{14}s_{23}s_{34}} + \frac{(s_{13}s_{14} + 2s_{12}(s_{14} + s_{23}) + s_{23}s_{24})s_{34}}{64s_{12}s_{14}s_{23}}. \tag{C8}$$

[1] S. Dawson, Nucl. Phys. **B359**, 283 (1991).

[2] A. Djouadi, M. Spira, and P. M. Zerwas, Phys. Lett. B **264**, 440 (1991).

[3] V. Del Duca, A. Frizzo, and F. Maltoni, J. High Energy Phys. 05 (2004) 064.

[4] L. J. Dixon, E. W. N. Glover, and V. V. Khoze, J. High Energy Phys. 12 (2004) 015.

[5] S. D. Badger, E. W. N. Glover, and V. V. Khoze, J. High Energy Phys. 03 (2005) 023.

[6] V. Del Duca, W. Kilgore, C. Oleari, C. Schmidt, and D. Zeppenfeld, Phys. Rev. Lett. **87**, 122001 (2001).

[7] V. Del Duca, W. Kilgore, C. Oleari, C. Schmidt, and D. Zeppenfeld, Nucl. Phys. **B616**, 367 (2001).

[8] D. Zeppenfeld, R. Kinnunen, A. Nikitenko, and E. Richter-Was, Phys. Rev. D **62**, 013009 (2000).

[9] A. Djouadi, hep-ph/0503172.

[10] R. V. Harlander, Phys. Lett. B **492**, 74 (2000).

[11] C. Anastasiou and K. Melnikov, Nucl. Phys. **B646**, 220 (2002).

[12] C. R. Schmidt, Phys. Lett. B **413**, 391 (1997).

[13] V. Ravindran, J. Smith, and W. L. Van Neerven, Nucl. Phys. **B634**, 247 (2002).

[14] R. P. Kauffman, S. V. Desai, and D. Risal, Phys. Rev. D **55**, 4005 (1997); **58**, 119901(E) (1998).

[15] M. L. Mangano, S. J. Parke, and Z. Xu, Nucl. Phys. **B298**, 653 (1988).

[16] F. A. Berends and W. T. Giele, Nucl. Phys. **B306**, 759 (1988).

[17] Z. Bern and D. A. Kosower, Nucl. Phys. **B362**, 389 (1991).

[18] G. 't Hooft and M. J. G. Veltman, Nucl. Phys. **B44**, 189 (1972).

[19] Z. Bern, A. De Freitas, L. J. Dixon, and H. L. Wong, Phys. Rev. D **66**, 085002 (2002).

[20] Z. Bern and D. A. Kosower, Nucl. Phys. **B379**, 451 (1992).

[21] Z. Kunszt, A. Signer, and Z. Trocsanyi, Nucl. Phys. **B411**, 397 (1994).

[22] S. Catani, M. H. Seymour, and Z. Trocsanyi, Phys. Rev. D **55**, 6819 (1997).

[23] W. T. Giele and E. W. N. Glover, J. High Energy Phys. 04 (2004) 029.

[24] P. Nogueira, J. Comput. Phys. **105**, 279 (1993).

[25] J. A. M. Vermaseren, math-ph/0010025.

[26] A. I. Davydychev, Phys. Lett. B **263**, 107 (1991).

[27] A. van Hameren, J. Vollinga, and S. Weinzierl, Eur. Phys. J. C **41**, 361 (2005).

[28] R. K. Ellis, W. T. Giele, and G. Zanderighi, hep-ph/0508308.

[29] T. Binoth, J. P. Guillet, G. Heinrich, E. Pilon, and C. Schubert, hep-ph/0504267.

[30] T. Binoth, G. Heinrich, and N. Kauer, Nucl. Phys. **B654**, 277 (2003).

[31] A. Ferroglia, M. Passera, G. Passarino, and S. Uccirati, Nucl. Phys. **B650**, 162 (2003).

[32] A. Andonov *et al.*, hep-ph/0411186.

[33] G. Belanger, F. Boudjema, J. Fujimoto, T. Ishikawa, T. Kaneko, K. Kato, and Y. Shimizu, hep-ph/0308080.

[34] E. de Doncker, Y. Shimizu, J. Fujimoto, F. Yuasa, K. Kaugars, L. Cucos, and J. Van Voorst, Nucl. Instrum. Methods Phys. Res., Sect. A **534**, 269 (2004).

[35] Z. Nagy and D. E. Soper, J. High Energy Phys. 09 (2003) 055.

[36] F. del Aguila and R. Pittau, J. High Energy Phys. 07 (2004) 017.

[37] W. Giele, E. W. N. Glover, and G. Zanderighi, Nucl. Phys. B Proc. Suppl. **135**, 275 (2004).

[38] Z. Bern, L. J. Dixon, and D. A. Kosower, Nucl. Phys. **B513**, 3 (1998).